Encirclement Control for UAV Target Tracking Based on Distance Measurement

Hailong Lv*
Unit 96815 of PLA, Jingdezhen, China
1056478033@qq.com

Xiaoyong Yao
Unit 96815 of PLA, Jingdezhen, China
17707984580@163.com

Jianhui Yuan
Unit 96815 of PLA, Jingdezhen, China
miobellroll@126.com

Jiangbo Jia
College of Automation Engineering, Nanjing University of Aeronautics and Astronautics, Nanjing, China
jiajiangbo@nuaa.edu.cn

Bo Yang
Unit 96815 of PLA, Jingdezhen, China
yang_bo_nudt@163.com

ABSTRACT

This paper investigates an encirclement control method of single unmanned aerial vehicle (UAV) for target tracking, which is based on the nonvanishing perturbation system stability analysis method. Different from the previous methods, we use distance measurement between the UAV and the target to design the guidance law instead of the coordinate information. It is proved by static mathematics that the guidance law is global uniformly asymptotically stable. The simulation shows that the guidance law can make the UAV track stationary or moving static stably and efficiently.

CCS CONCEPTS

• **Computing methodologies** → Artificial intelligence; Control methods; Computational control theory.

KEYWORDS

Encirclement control, UAV, Nonvanishing perturbation system, Guidance law, Distance measurement

ACM Reference Format:
Hailong Lv*, Xiaoyong Yao, Jianhui Yuan, Jiangbo Jia, and Bo Yang. 2021. Encirclement Control for UAV Target Tracking Based on Distance Measurement. In *2021 International Conference on Mechanical, Aerospace and Automotive Engineering (CMAAE 2021), December 03–05, 2021, Changsha, China.* ACM, New York, NY, USA, 6 pages. https://doi.org/10.1145/3518781.3519198

1 INTRODUCTION

Target tracking with UAVs has been widely used in military and civilian fields, such as patrol and reconnaissance, transportation protection and auxiliary positioning, etc., and has attracted considerable research attention in recent decades. Typical tracking methods include overhead tracking [1-3] and encirclement tracking [4-6]. Encirclement tacking aims to design a guidance law to make the UAV move on a circular track at a certain distance from the target [7-10].

Many efforts have been devoted to the study of UAV encirclement tracking. Fei Dong [4] purpose a guidance law based on range measurements to encircle the target with zero steady-state error for any desired smooth pattern. M. E. Campbell [11] proposed a cooperative tracking approach for UAV with camera which utilizes a square root sigma point information filter. Zhang, Meng, and Yang [12] proposed an improved Lyapunov guided vector field based on chaos theory to avoid the fixed path that is easy to be detected when the UAV is tracking the target. T. Z. Muslimov [10] proposed a fixed-wing UAV guidance law based on Lyapunov non-uniform in both magnitude and direction path-following vector field and considered input constraints. Cao [9] [13] [14] designed guidance laws for encirclement tracking based on the position obtained by GPS, the distance obtained by sensors, and rate changes of the UAV, respectively. A. S. Matveev [15] proposed a three-dimensional tracking guidance law. Xiao Y [7] [8] [16] designed some control method for nonholonomic vehicle based on the theory of nonlinear systems, which has brought inspiration to our work. This paper develops some ideas form Matveev [17-20], who proposed some control method based on distance measurements for mobile robots. Inspired by the existing research, a lemma of the stability of a nonvanishing perturbation system is proposed. Based on this lemma, a guidance law using UAV distance measurement instead of location information is proposed for target encirclement tracking.

This paper is organized as follows. In section 2, the UAV dynamic model and nonvanishing perturbation lemma are given. Section 3 proposes a distance-based guidance law and proves its stability. In section 4, the simulation results are shown to illustrate the main result. In section 5, the conclusions are drawn.

2 PRELIMINARIES

In this section, we will give the dynamics model of the UAV and a technical lemma that will be used instability analysis of the system.

2.1 Problem Formulation

First, we use the Dubins vehicle model to describe the guidance problem of a single UAV tracking ground target in a two-dimensional plane. This model is also called a single-wheel model and is usually used as a mass point kinematics model. Its kinematics is described

Permission to make digital or hard copies of all or part of this work for personal or classroom use is granted without fee provided that copies are not made or distributed for profit or commercial advantage and that copies bear this notice and the full citation on the first page. Copyrights for components of this work owned by others than ACM must be honored. Abstracting with credit is permitted. To copy otherwise, or republish, to post on servers or to redistribute to lists, requires prior specific permission and/or a fee. Request permissions from permissions@acm.org.
CMAAE 2021, December 03–05, 2021, Changsha, China
© 2021 Association for Computing Machinery.
ACM ISBN 978-1-4503-8520-6/21/12…$15.00
https://doi.org/10.1145/3518781.3519198

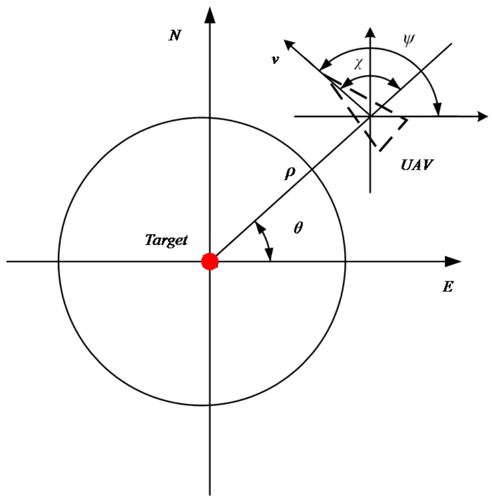

Figure 1: The Geometric of the Target Encirclement Tracking

as follows:

$$\begin{cases} \dot{x} = v\cos\psi \\ \dot{y} = v\sin\psi \\ \dot{\psi} = \omega \end{cases} \tag{1}$$

where $p = [x, y]^T \in R^2$, $\psi \in [0, 2\pi]$, $\omega \in R$, and $v \in R$ denote the 2D position, heading angle, angular speed, and linear speed of the UAV, respectively. Define $p_t = [x_t, y_t]^T \in R^2$ as the 2D location of the target. The range between the UAV and target can be defined as $\rho = \sqrt{[x(t) - x_t(t)]^2 + [y(t) - y_t(t)]^2} \in R^+$.

The geometric of the target encirclement tracking is shown in 1

The dynamic can be changed from the Cartesian coordinates system to the polar coordinate system. Then, the UAV dynamics (1) can be transformed into the following form:

$$\begin{cases} \dot{\rho} = -v\cos\chi \\ \dot{\chi} = \omega + \frac{v}{\rho}\sin\chi \end{cases} \tag{2}$$

where χ_i denotes the bearing angle. $\chi_i = \pi/2$ and $\chi_i = 3\pi/2$ represent the clockwise and counterclockwise motions of the UAV, respectively. In dynamics (2), the state variables are transformed from $[\ x \quad y \quad \psi\ ]^T$ to $[\ \rho \quad \chi\ ]^T$.

The following physical velocity constraints are considered:

$$v \in [v_{\min}, v_{\max}], 0 < v_{\min} < v_{\max} \tag{3}$$

$$\omega \in [-\omega_{\max}, \omega_{\max}], \omega_{\max} > 0 \tag{4}$$

In this paper, the location p_t of the target is unknown. All the angles and distances are measured by the sensor, such as radar or infrared measuring instruments, etc., which will not be discussed. To facilitate the analysis, we assume that the UAVs only adopt the clockwise motion. The situation of counterclockwise motion can be analyzed in the same way.

2.2 A Technical Lemma

Consider the following system:

$$\dot{z} = f(t, z) + g(t, z) \tag{5}$$

where $z \in R^n$, denote state vectors of the overall system. $f(t, z)$ and $g(t, z)$ are continuous in their arguments. $f(t, z)$is locally Lipschitz on t_d uniformly on z_d and $g(t, z)$ is locally Lipschitz on z_d. The system (5) can be viewed as a perturbation of the normal system.

$$\dot{z} = f(t, z) \tag{6}$$

Lemma 1 Let $t = t_d$ be an equilibrium point for the system (5). If conditions [C1] – [C3] are satisfied. The system (5) is globally uniformly asymptotically stable at $t = t_d$.

[C1] The nominal system (6) is globally uniformly asymptotically stable with a Lyapunov function $V(t, z)$

$$\frac{\partial V}{\partial t} + \frac{\partial V}{\partial z} f(t, z) \le -c_1\varphi^2(z) \tag{7}$$

$$\left\| \frac{\partial V}{\partial z} \right\| \le c_2\varphi(z) \tag{8}$$

$$\|g(t, z)\| \le \gamma\varphi(z) \tag{9}$$

[C2] α and β are positive constants, $\|\varphi(z)\|$ is a class K function.

[C3] The perturbation term satisfies the bound:

$$\gamma < \frac{c_1}{c_2} \tag{10}$$

The proof can be found in reference [20]. **Lemma 1** is stated for the case when the equilibrium point at the origin. The origin can be shifted to any equilibrium point via a change of variables without any loss of generality.

3 MAIN RESULT

3.1 Guidance Law Design

To achieve the purpose of target encirclement tracking, we propose the following guidelines based on the distance and angle information obtained by the UAV sensor:

$$\begin{cases} \omega = \begin{bmatrix} k_\omega \left[\frac{\tanh^2(\rho - \rho_d)}{\cos\chi} + \cos\chi \right] \\ + \tanh(\rho - \rho_d) - \frac{\sin\chi}{\rho} \end{bmatrix} v_d \\ v = v_d + k_v\rho\left[\tanh(\rho - \rho_d) + \cos\chi\right] \end{cases} \tag{11}$$

where k_ω and k_v are positive constants.

Substitute the guidance law (11) into the system (2) to form a closed loop system which is nonlinear composite:

$$\begin{cases} \dot{\rho} = -v_d\cos\chi \\ \dot{\chi} = k_\omega \left[\frac{\tanh^2(\rho - \rho_d)}{\cos\chi} + \cos\chi \right] v_d \\ \quad + \tanh(\rho - \rho_d) v_d \\ + k_v \sin\chi \left[\tanh(\rho - \rho_d) + \cos\chi\right] \end{cases} \tag{12}$$

According to **Lemma 1**, the nonlinear composite system (12) describes the system status of the UAV. The system can decompose into a nominal subsystem term $f(t, z)$ and a perturbation term $g(t, z)$ as follows:

$$f(t, z) = \begin{bmatrix} -v_d\cos\chi \\ \begin{Bmatrix} k_\omega \left[\frac{\tanh^2(\rho - \rho_d)}{\cos\chi} + \cos\chi \right] v_d \\ + \tanh(\rho - \rho_d) v_d \end{Bmatrix} \end{bmatrix} \tag{13}$$

$$g(t,z) = \begin{bmatrix} -k_v \rho \cos\chi \left[\tanh(\rho - \rho_d) + \cos\chi\right] \\ k_v \sin\chi \left[\tanh(\rho - \rho_d) + \cos\chi\right] \end{bmatrix} \tag{14}$$

Theorem 1 The composite system (12) is globally uniformly asymptotically stable at its equilibrium point$z_1 = \begin{bmatrix} \rho_d & \frac{\pi}{2} \end{bmatrix}^T$ and $z_2 = \frac{2\pi}{N}$.

3.2 Proof of the Theorem 1

In this section, we will prove the stability of each subsystem (13) and (14) according to the stability proof method of **Lemma1**.

For the nominal part of the system, the following Lyapunov equation is proposed.

$$V(t,z) = \ln\cosh(\rho - \rho_d) + 1 - \sin\chi \tag{15}$$

1) Taking the time derivative yields:

$$\begin{aligned} \frac{\partial V}{\partial t} &= \frac{\partial[\ln\cosh(\rho-\rho_d)+1-\sin\chi]}{\partial t} \\ &= \tanh(\rho - \rho_d)\dot{\rho} - \dot{\chi}\cos\chi \\ &= \tanh(\rho - \rho_d)(-v_d \cos\chi_i) \\ &- \cos\chi k_\omega \left[\frac{\tanh^2(\rho-\rho_d)}{\cos\chi} + \cos\chi\right] v_d \\ &- \cos\chi\left[-\tanh(\rho - \rho_d)\right] v_d \\ &= -k_\omega v_d \left[\tanh^2(\rho - \rho_d) + \cos^2\chi\right] \end{aligned}$$

and

$$\begin{aligned} \frac{\partial V}{\partial z} f(z) &= \frac{\partial[\ln\cosh(\rho-\rho_d)+1-\sin\chi]}{\partial z} f(z) \\ &= \begin{bmatrix} \tanh(\rho - \rho_d) \\ -\cos\chi \end{bmatrix} \begin{bmatrix} -v_d \cos\chi_i \\ \begin{bmatrix} k_\omega \left[\frac{\tanh^2(\rho-\rho_d)}{\cos\chi} + \cos\chi\right] \\ -\tanh(\rho - \rho_d) \end{bmatrix} v_d \end{bmatrix} \\ &= -k_\omega v_d \left[\tanh^2(\rho - \rho_d) + \cos^2\chi\right] \end{aligned}$$

Therefore,

$$\begin{aligned} &\frac{\partial V}{\partial t} + \frac{\partial V}{\partial z} f(z) \\ &= -2k_\omega v_d \left[\frac{1}{2}\left(\frac{1}{\rho} - \frac{1}{\rho_d}\right)^2 + (1 - \sin\chi)^2\right] \end{aligned} \tag{16}$$

We can get

$$c_1 = 2k_\omega v_d \tag{17}$$

2) The norm of the derivation of V to z:

$$\left\| \frac{\partial V_1}{\partial z} \right\| = \sqrt{\tanh^2(\rho - \rho_d) + \cos^2\chi}$$

It can be obtained that

$$c_2 = 1 \tag{18}$$

3) For the perturbation term $g_1(z_1, z_2)$ of the system:

$$\begin{aligned} &\|g(t,z)\| \\ &\le k_v \sqrt{(\rho^2\cos^2\chi + \sin^2\chi)\left[\tanh(\rho - \rho_d) + \cos\chi\right]^2} \\ &\le k_v \sqrt{2\left(\rho_{\max}^2 + 1\right)}\sqrt{\tanh^2(\rho - \rho_d) + \cos^2\chi} \end{aligned}$$

Thus,

$$\gamma = k_v \sqrt{2\left(\rho_{\max}^2 + 1\right)} \tag{19}$$

Obviously, if $\rho_{\max} < \sqrt{2\frac{{k_\omega}^2}{{k_v}^2} {v_d}^2 - 1}$, $\dot{V}(t,z)$ is negative definite. From Lemma 1, the system (13) is globally uniformly asymptotically stable at $\rho = \rho_d$ and $\chi = \frac{\pi}{2}$.

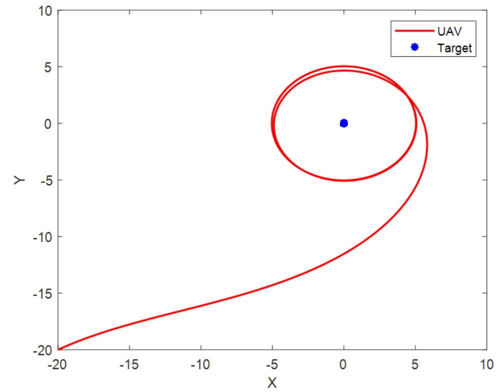

Figure 2: Trajectory for Stationary Target

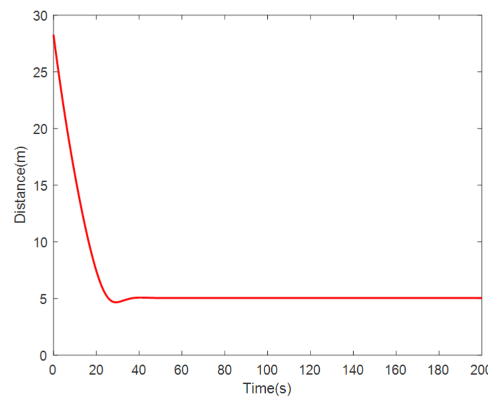

Figure 3: Distance Between UAVs and the Stationary Target

4 SIMULATION

Consider a UAV encircling and tracking a target, as shown in Fig. 1. By default, all variables are in SI units. This article does not consider collision avoidance, so the simulation is in a rational non-collision environment. In the simulation, the targets are stationary and moving, respectively.

4.1 Stationary Target

When the target is stationary, the UAV starts from a random position and arrives on an orbit $\rho = \rho_d$ from the target to achieve encircling and tracking. The initial state of the target and the drone is shown in Table 1. We assume $v \in [0.5, 5.8]$, $\omega \in [-0.6, 0.6]$, desired encirclement distance $\rho_d = 5$, and desired velocity $v_d = 1.5$.

The algorithms were implemented in MATLAB R2020b, and the simulation lasted for 200s with a step length of 0.05s.

2 shows the trajectories of the UAV for encircling and tracking a stationary target. 2–6 show the status changes of the UAV while encircling and tracking the stationary target. As we can see, when the UAV is stable, the distance between the UAV with target and the bearing angle of the UAV reached the stable point $\begin{bmatrix} \rho & \chi \end{bmatrix}^T = \begin{bmatrix} 5 & \frac{\pi}{2} \end{bmatrix}$. Angular velocity and linear velocity of the

Table 1: Initial States for Stationary Target

Name	Initial states	
	Position	*Heading angle*
Target	(0, 0)	0
UAV	(-20, -20)	$\frac{\pi}{6}$

Table 2: The Design Parameters of The UAV at Each Stage

Design Parameters	*Stage 1*	*Stage 2*	*Stage 3*
Speed	15	18	20
ρ_d	250	200	300

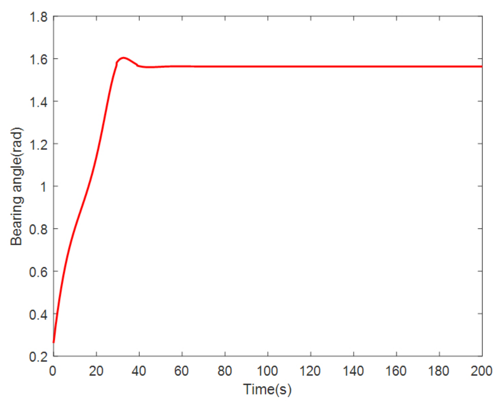

Figure 4: Bearing Angle of the UAV

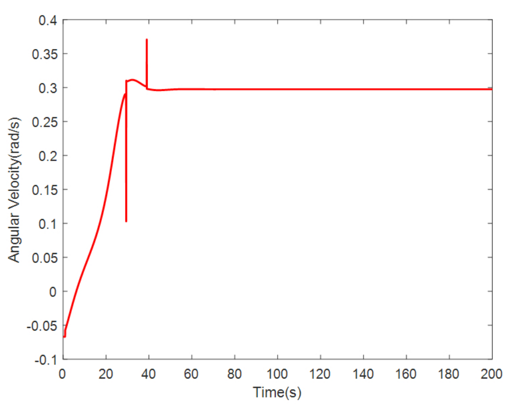

Figure 5: Angular Velocity of the UAV

UAV converge to 0.3 (5) and 1.5 (6). This simulation verifies the proposed guidance law (12) can be applied to encircle and track the stationary target.

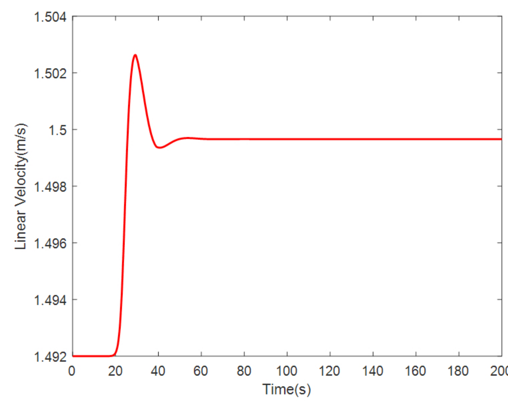

Figure 6: The Linear Velocity of the UAV

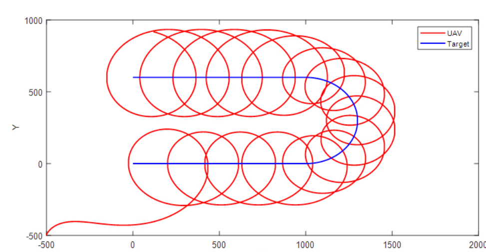

Figure 7: Trajectory of the UAV for Moving Target

4.2 Moving Target

In this section, the movement of the target is divided into three stages. The speed and encirclement radius of each stage are shown in Table 2. The initial position and heading angle of the UAV are $(-500, -500)$ and $\frac{\pi}{2}$. The initial position of the target is $(0, 0)$, same as the previous section. We assume $v \in [10, 22]$, $\omega \in [-0.6, 0.6]$.

The algorithms were implemented in MATLAB R2020b, and the simulation lasted for 1500s with a step length of 0.05s.

7 shows the trajectories of the UAV for encircling and tracking a moving target. It can be seen that although each stage has different requirements, the UAV can track the target stably. 811 show the

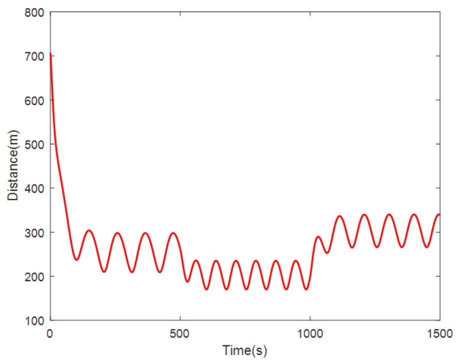

Figure 8: Distance between UAVs and the Moving Target

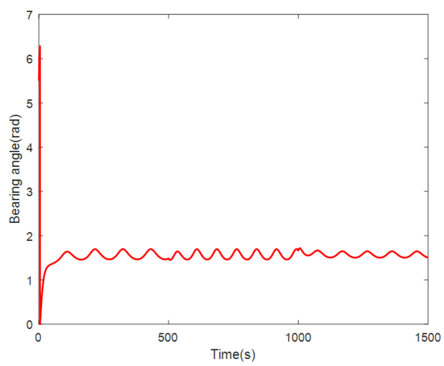

Figure 9: Bearing Angle of the UAV for Moving Target

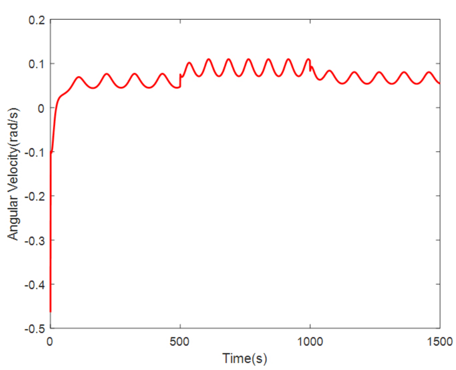

Figure 10: Angular Velocity of the UAV for Moving Target

status changes of UAV for the moving target. As we can see, the UAV can converge to the expected value, but the curve is oscillating. In the next work, we can use the target's moving speed as a reference for the guidance law to eliminate shocks. On the whole, the proposed guidance law can be used for encircling and tracking a moving target.

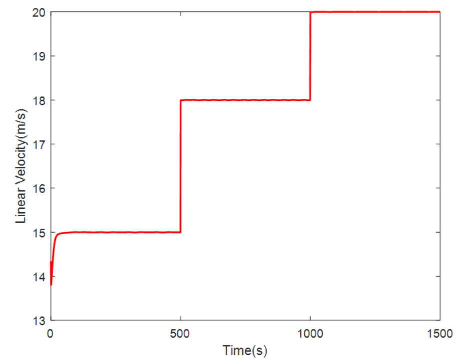

Figure 11: Linear Velocity of the UAV for Moving Target

5 CONCLUSION

In this paper, we have proposed a guidance law for encirclement control of the target tracking by a single UAV using distance measurement. Different from the existing methods, the guidance laws of angular velocity and linear velocity are verified in the nonvanishing perturbation rather than proved separately. It is closer to reality. The constraints of linear and angular velocity are also taken into account, which is conducive to the application of our guidance law to fixed-wing UAVs and other aircraft with minimum speed restrictions. In the future work, we will consider the interference to the system by reducing the target speed, and consider UAV collision avoidance to better track moving targets at the same time.

REFERENCES

[1] D. N. Cardoso, S. Esteban, and G. V. Raffo, "A new robust adaptive mixing control for trajectory tracking with improved forward flight of a tilt-rotor UAV," ISA Transactions, vol. 110, pp. 86-104, 2021

[2] H. Liu, Y. Lyu, and W. Zhao, "Robust visual servoing formation tracking control for quadrotor UAV team," Aerospace Science and Technology, vol. 106, p. 106061, 2020,

[3] D. Chwa, "Nonlinear Tracking Control of 3-D Overhead Cranes Against the Initial Swing Angle and the Variation of Payload Weight," IEEE Transactions on Control Systems Technology, vol. 17, no. 4, pp. 876-883, 2009

[4] F. Dong, K. You, and S. Song, "Target encirclement with any smooth pattern using range-based measurements," Automatica, vol. 116, p. 108932, 2020,

[5] L. Briñón-Arranz, A. Seuret, and A. Pascoal, "Circular formation control for cooperative target tracking with limited information," Journal of the Franklin Institute, vol. 356, no. 4, pp. 1771-1788, 2019.

[6] Y. Xie, L. Han, X. Dong, Q. Li, and Z. Ren, "Bio-inspired adaptive formation tracking control for swarm systems with application to UAV swarm systems," Neurocomputing, vol. 453, pp. 272-285, 2021.

[7] X. Yu, X. Xu, L. Liu, and G. Feng, "Circular formation of networked dynamic unicycles by a distributed dynamic control law," Automatica A Journal of Ifac the International Federation of Automatic Control, vol. 89, pp. págs. 1-7, 2018.

[8] X. Yu, N. Ding, A. Zhang, and H. Qian, "Cooperative Moving-Target Enclosing of Networked Vehicles With Constant Linear Velocities," IEEE Trans Cybern, vol. 50, no. 2, pp. 798-809, Feb 2020,.

[9] Y. Cao, D. Casbeer, D. Milutinovic, and D. Kingston, "Collective Circular Motion and Cooperative Circumnavigation for Nonholonomic Mobile Robots Using Range-based Measurements," in Aiaa Guidance, Navigation, & Control Conference, 2016.

[10] T. Z. Muslimov and R. A. Munasypov, "Adaptive decentralized flocking control of multi-UAV circular formations based on vector fields and backstepping," ISA Transactions, vol. 107, pp. 143-159, 2020.

[11] M. E. Campbell and W. W. Whitacre, "Cooperative Tracking Using Vision Measurements on SeaScan UAVs," IEEE Transactions on Control Systems Technology, vol. 15, no. 4, pp. 613-626, 2007.

[12] Y. Zhang, Q. Meng, and X. Yang, "2D plane standoff tracking based on Chaos-Lyapunov guidance vector field," in 2017 29th Chinese Control And Decision Conference (CCDC), 28-30 2017, pp. 1291-1294.

[13] Y. Cao, "UAV Circumnavigating an Unknown Target Under a GPS-denied Environment with Range-only Measurements," Automatica, vol. 55, 2015.
[14] A. Hashemi, Y. Cao, D. W. Casbeer, and G. Yin, "Unmanned Aerial Vehicle Circumnavigation Using Noisy Range-Based Measurements Without Global Positioning System Information," Journal of Dynamic Systems Measurement & Control, vol. 137, no. 3, 2015.
[15] A. S. Matveev and A. A. Semakova, "Localization and Three-Dimensional Circumnavigation of Many Mobile Targets ‹Based on Distance Measurements**This work was supported by the Russian Science Foundation (Proj. No 14-21-00041p)," IFAC-PapersOnLine, vol. 50, no. 1, pp. 8832-8837, 2017,.
[16] X. Yu and L. Liu, "Cooperative Control for Moving-Target Circular Formation of Nonholonomic Vehicles," IEEE Transactions on Automatic Control, vol. 62, no. 7, pp. 3448-3454, 2017.
[17] A. S. Matveev, H. Teimoori, and A. V. Savkin, "Range-only measurements based target following for wheeled mobile robots," Automatica, vol. 47, no. 1, pp. 177-184, 2011.
[18] A. S. Matveev, M. C. Hoy, and A. V. Savkin, "3D environmental extremum seeking navigation of a nonholonomic mobile robot," Automatica, vol. 50, no. 7, pp. 1802-1815, 2014.
[19] A. S. Matveev, A. A. Semakova, and A. V. Savkin, "Range-only based circumnavigation of a group of moving targets by a non-holonomic mobile robot," Automatica, vol. 65, pp. 76-89, 2016.
[20] [A. S. Matveev, H. Teimoori, and A. V. Savkin, "Navigation of a unicycle-like mobile robot for environmental extremum seeking," Automatica, vol. 47, no. 1, pp. 85-91, 2011.